

CONTROLLED DENSIFICATION OF MULLITE FOR COMPOSITE APPLICATIONS*

T. A. Cruse, B. J. Polzin, P. J. Phelan, D. Singh, and K. C. Goretta

Energy Technology Division
Argonne National Laboratory, Argonne IL 60439-4838, USA

A. R. de Arellano-López
Dept. de Fisica de la Materia Condensada
Universidad de Sevilla, Sevilla 41080, Spain

April 1999

The submitted manuscript has been created by the University of Chicago as Operator of Argonne National Laboratory ("Argonne") under Contract No. W-31-109-ENG-38 with the U.S. Department of Energy. The U.S. Government retains for itself, and others acting on its behalf, a paid-up, nonexclusive, irrevocable worldwide license in said article to reproduce, prepare derivative works, distribute copies to the public, and perform publicly and display publicly, by or on behalf of the Government.

RECEIVED
SEP 28 1999
QSTI

Submitted to Proceedings of 101st Annual Meeting of the American Ceramic Society, April 22-24, 1999, Indianapolis, IN.

*Work supported by the Defense Advanced Research Projects Agency, through a Department of Energy Interagency Agreement, and Work for Others Contract 82110, under Contract W-31-109-Eng-38.

DISCLAIMER

This report was prepared as an account of work sponsored by an agency of the United States Government. Neither the United States Government nor any agency thereof, nor any of their employees, make any warranty, express or implied, or assumes any legal liability or responsibility for the accuracy, completeness, or usefulness of any information, apparatus, product, or process disclosed, or represents that its use would not infringe privately owned rights. Reference herein to any specific commercial product, process, or service by trade name, trademark, manufacturer, or otherwise does not necessarily constitute or imply its endorsement, recommendation, or favoring by the United States Government or any agency thereof. The views and opinions of authors expressed herein do not necessarily state or reflect those of the United States Government or any agency thereof.

DISCLAIMER

**Portions of this document may be illegible
in electronic image products. Images are
produced from the best available original
document.**

CONTROLLED DENSIFICATION OF MULLITE FOR COMPOSITE APPLICATIONS

T. A. Cruse, B. J. Polzin, P. J. Phelan, D. Singh, and K. C. Goretta
Energy Technology Division
Argonne National Laboratory, Argonne, IL 60439-4838, U.S.A.

A. R. de Arellano-López
Dept. de Fisica de la Materia Condensada
Universidad de Sevilla, Sevilla 41080, Spain

ABSTRACT

As part of an effort to fabricate oxide-based fibrous monolithic ceramics, sintering of mullite has been examined. The effects of Y_2O_3 additions on sinterability of sol-gel-derived mullite and on the resulting microstructures were evaluated over a range of compositions, sintering times, and temperatures. Electron microscopy, X-ray diffraction, differential thermal analysis, and density measurements indicated that the Y_2O_3 additions promoted densification through formation of a Y-Si-Al-O liquid phase. This phase tended to solidify as a glass during normal processing, but could be crystallized by a two-step annealing process at 1300 and 1200°C. The four-point flexural strengths of mullite and mullite-5 wt.% Y_2O_3 were also examined.

INTRODUCTION

Development of ceramic fibrous monoliths (FMs) has been the primary goal of our research to date. FMs typically consist of a strong, primary cell phase and a weaker, secondary cell-boundary phase [1-6]. The weaker phase may also serve as an interphase between the cell and a strong matrix in a three-constituent structure. This structure allows FMs to exhibit graceful failure and improved toughness compared to that of monolithic ceramics. Improved toughness and tolerance to flaws relies on several mechanisms; the primary mechanisms tend to be crack deflection through the cell-boundary phase and debonding between the two phases. In this manner, FMs are similar to traditional continuous fiber ceramic composites (CFCC). FMs differ from CFCCs in that they are produced in-situ by traditional powder-processing techniques and thus promise to be much

less expensive to produce [1-3].

Most of the work on FMs to date has been conducted on SiC/BN [4], Si₃N₄/BN [5,6], and cermets. These systems generally require high-temperature hot pressing to achieve good densification, and they oxidize at high temperature in air. Therefore, oxides that can be sintered to high density are of interest for FM applications.

Mullite appears to be an excellent candidate material for FMs. It offers a good combination of high-temperature properties: high strength and resistance to creep, chemical attack, and thermal shock. Sintering aids have been shown to lower the sintering temperature needed to produce a high-density mullite [7-11]. With a suitably doped mullite as the cell phase and an undoped mullite as the cell-boundary phase, it should be possible to produce a highly dense cell and weaker, less-dense cell boundary. Such an FM structure should be capable of dissipating energy during fracture.

Based on a review of literature [7-11] and some preliminary evaluations, Y₂O₃ was selected as the sintering aid. Sintering aids generally improve the densification of mullite through liquid-phase sintering. TiO₂ is reported to improve the densification of diphasic mullite gels by lowering the viscosity of an intermediate glass phase, resulting in improved densification [7]; however, anisotropic grain growth can result. Y₂O₃ is expected to improve densification in a similar manner. Recent work on the SiO₂-Al₂O₃-Y₂O₃ phase diagram confirms formation at common sintering temperatures of a liquid phase [12]. Under equilibrium conditions, this phase will transform upon cooling to Y₂Si₂O₇, mullite, and Al₂O₃. Y₂O₃ has also been used as an effective sintering aid for Si₃N₄ [13-15]. Work has shown that crystallization of the Y₂Si₂O₇ phase in Si₃N₄ imparted improved strength compared to Si₃N₄ with an amorphous Y₂Si₂O₇ phase [14]. Similar results may be possible for the Y₂Si₂O₇ phase in mullite.

EXPERIMENTAL PROCEDURES

Mullite was produced by a colloidal sol-gel approach. Colloidal SiO₂ (Alfa Aesar, particle size \approx 0.02 μ m) was used to prepare a SiO₂ sol and boehmite (γ -AlOOH, Alcoa Hi-Q 10) was used to prepare an Al₂O₃ sol. Y₂O₃ (Sigma Aldrich Corp., particle size \approx 1 μ m) was added to the Al₂O₃ sol. Sintering aid concentrations were 0-15 wt.% of the final product. The sols were mixed together and HNO₃ was added to produce a pH of 3. The sol was gelled by heating in air at 80°C for 24 h. The gel was ground and calcined in air at 1000°C for 2 h. The calcined material was ball-milled for 24 h in isopropyl alcohol. The resulting material was then dried and sieved.

The powder was then uniaxially pressed at 175 MPa in a 1.27-cm cylindrical die. The resulting specimens were then fired for various times (0-12 h) at 1550°C and for 3 h at various temperatures (1400-1650°C). Some specimens were then

annealed at 1300°C for 24 h, then cooled to 1200°C and held for another 24 h, in an attempt to crystallize an amorphous grain boundary phase.

After firing, densities were determined by geometric and Archimedes methods; agreement was typically within 1%. Specimens were then cut and polished with diamond paste to a 1- μm finish. The polished specimens were then thermally etched, typically at 100°C below the sintering temperature. Scanning electron microscopy (SEM) and transmission electron microscopy (TEM) photomicrographs were used for microstructural analysis; energy-dispersive analysis of X-rays (EDS) was used to determine elemental compositions.

Bars of some materials were also prepared by uniaxially pressing to 51 MPa and sintering at 1550°C for 3 h. These bars were used for four-point flexural strength measurements and thermomechanical analysis to determine the coefficient of thermal expansion. Several specimens were examined by X-ray diffraction (XRD) and differential thermal analysis (DTA).

$\text{Y}_2\text{Si}_2\text{O}_7$ was prepared by mixing Y_2O_3 and colloidal SiO_2 . The material was dried, ball-milled for 24 h in isopropyl alcohol, redried, sieved, and pressed into specimens. Bars were prepared by uniaxially pressing to 51 MPa and sintering at 1200 or 1550°C for 3 h. The goal of the different temperatures was to produce α -phase and γ -phase $\text{Y}_2\text{Si}_2\text{O}_7$.

RESULTS AND DISCUSSION

Y_2O_3 additions ranging from 1 to 15 wt.% were examined to determine effects on microstructural development with sintering in air at 1550°C for 3 h. All concentrations induced significant improvement in densification compared to that of pure mullite. For Y_2O_3 additions greater than 5 wt.%, there was a significant increase in grain growth, while concentrations less than 5 wt.% did not densify as quickly. Because our goal was to achieve rapid densification with minimal grain growth, 5 wt.% was selected.

After selecting mullite-5 wt.% Y_2O_3 as the best candidate material for our application, we conducted time and temperature studies to determine optimal processing conditions. Figure 1a shows the effect on density of sintering time at 1550°C. At 1550°C, most of the sintering occurred within the first 3 h for mullite-5 wt.% Y_2O_3 . Beyond this time, the density decreased slightly. For pure mullite, density continued to increase with increasing sintering time. Figure 1b shows the effect on density of sintering temperature; sintering time was 3 h. The maximum density for mullite-5 wt.% Y_2O_3 occurred at 1500°C, whereas with pure mullite, the density continued to increase with increasing sintering temperature.

The decrease in density observed with mullite-5 wt.% Y_2O_3 with longer sintering times and higher sintering temperatures coincides with an increase in anisotropic grain growth and an increase in porosity. Figure 2 provides a

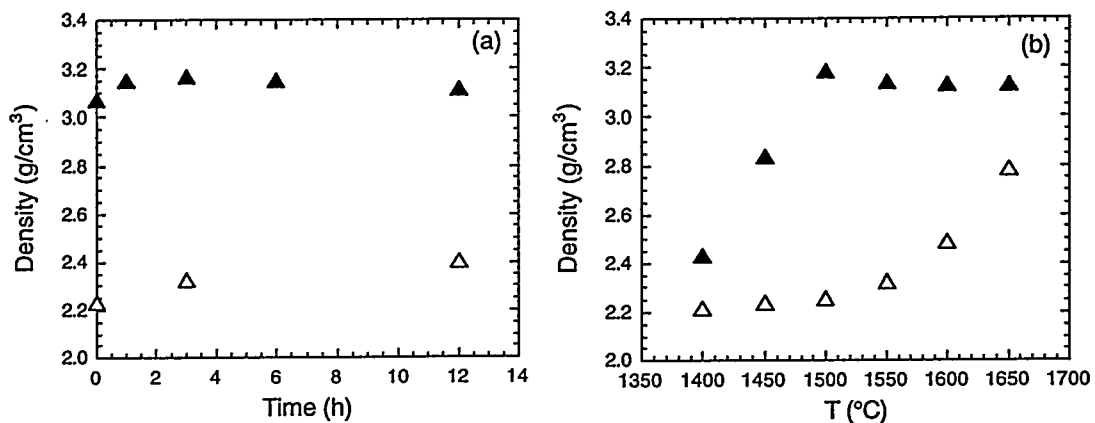


Figure 1. For mullite(Δ) and mullite-5 wt.% Y_2O_3 (\blacktriangle): (a) Effect of sintering time at 1550°C and (b) effect of temperature for sintering 3 h.

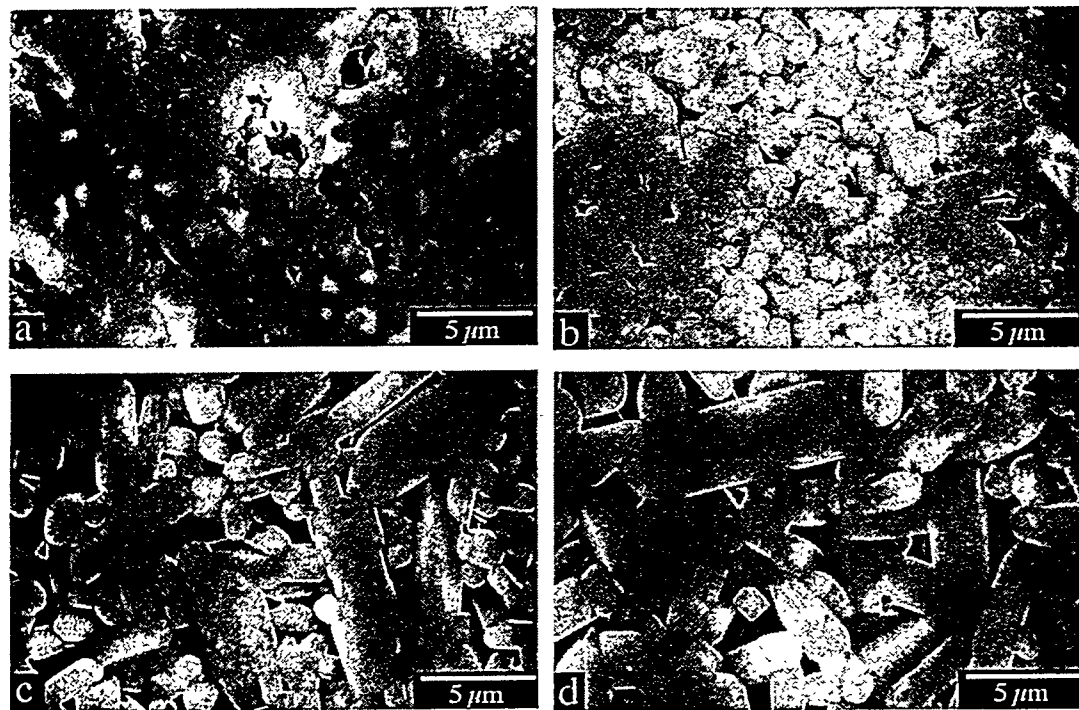


Figure 2. SEM photomicrographs of mullite-5wt.% Y_2O_3 specimens sintered for 3 h at (a) 1450, (b) 1500, (c) 1550, and (d) 1600°C.

comparison of the microstructures for different sintering temperatures. Changing the sintering temperature from 1500 to 1550°C caused a significant increase in grain size and aspect ratio. Figure 3 shows changes in microstructure resulting from different sintering times at 1550°C. There was change in grain size between the 3 h specimen and the 6 h specimen, as well as an increase in the size and concentration of porosity. These effects also coincided with a decrease in density.

Other considerations in the production of FMs include strength and coefficient of thermal expansion. The cell phase should be approximately an order of magnitude stronger than the cell-boundary phase to promote crack growth in the boundary phase and help limit crack growth into the cell phase. The room-temperature strength of 70%-dense mullite was \approx 34 MPa and that of >95%-dense mullite-5 wt.% Y_2O_3 was \approx 180 MPa. Further modifications to processing should improve the strength of the mullite-5 wt.% Y_2O_3 . For example, >95%-dense mullite doped with MgO was reported to have a room-temperature three-point flexural strength of 350 MPa [16]. With continued work, the Y_2O_3 -doped mullite may achieve a similar strength.

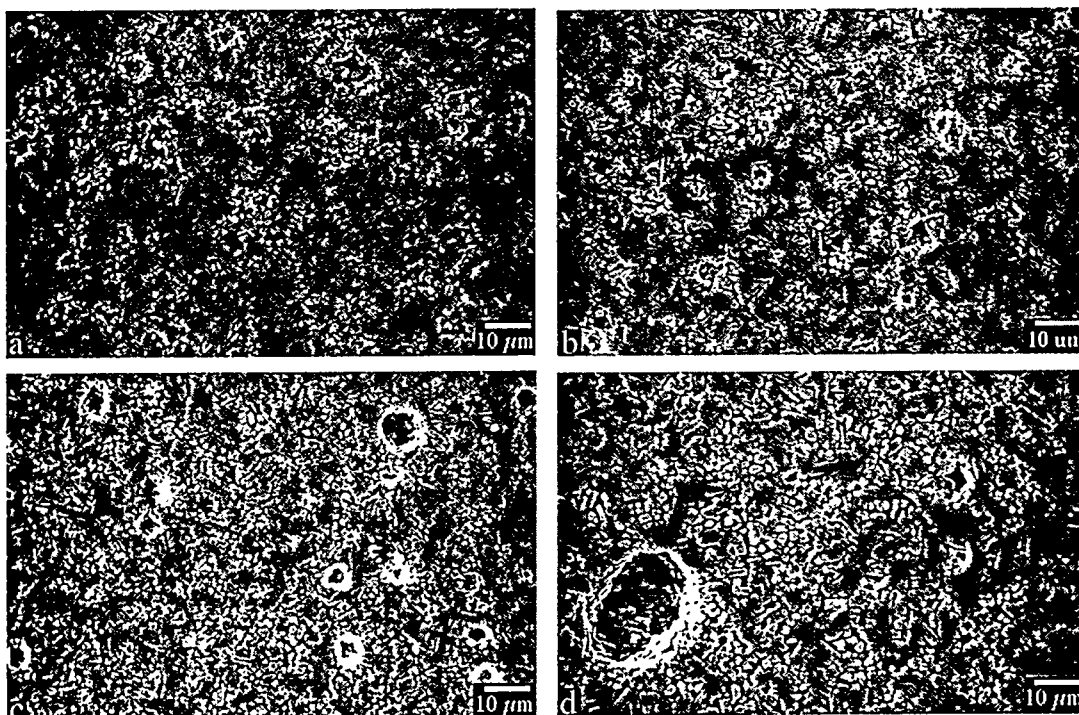


Figure 3. SEM photomicrographs comparing effects of sintering time at 1500°C on microstructure of mullite-5 wt.% Y_2O_3 specimens: (a) no hold, (b) 3 h, (c) 6 h, and (d) 12 h.

For FMs, all constituents should have similar coefficients of thermal expansion (α). Values of α were obtained by thermomechanical analysis for 65%-dense mullite and \approx 95%-dense mullite-5 wt.% Y_2O_3 . The average values of α from 25 to 1400°C were 5.9×10^{-6} cm/cm-°C and 6.2×10^{-6} cm/cm-°C, respectively. The slight change in the thermal expansion of mullite with the addition of Y_2O_3 or with large changes in density indicates that little internal stress should develop in cofired structures.

For the production of mullite-based FMs, sintering mullite/mullite-5 wt.% Y_2O_3 at 1500°C for 3 h should be nearly optimal. This should result in a strong cell phase that is nearly fully dense and a cell-boundary phase that is weaker and only \approx 70% dense. The density of the cell boundary phase may be further decreased by incorporating a combustible material such as carbon; this would also help to match shrinkages between the two phases during cosintering.

Further characterization of mullite-5 wt.% Y_2O_3 was conducted to better understand the sintering response of this material. Examination of the phase diagram by Kolitsch et al [12] indicates that the phases present in mullite-5 wt.% Y_2O_3 at room temperature should be mullite, Al_2O_3 , and $\text{Y}_2\text{Si}_2\text{O}_7$. XRD of mullite-5 wt.% Y_2O_3 produced under the standard conditions showed no indication of the presence of Al_2O_3 or a $\text{Y}_2\text{Si}_2\text{O}_7$. However, by annealing the material, XRD revealed the presence of β - $\text{Y}_2\text{Si}_2\text{O}_7$ (Fig. 4).

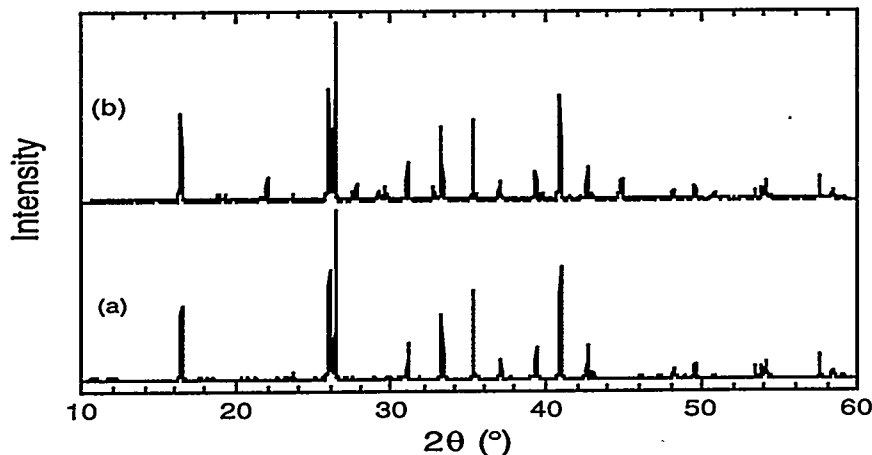


Figure 4. XRD of mullite-5 wt.% Y_2O_3 : (a) as sintered and (b) after annealing. In the as-sintered specimen, only mullite was detected, but after annealing, β - $\text{Y}_2\text{Si}_2\text{O}_7$ was also detected.

SEM examination of the surface of a mullite-5 wt.% Y_2O_3 pellet indicated the presence of a secondary phase, which EDS analysis revealed to have an approximate composition of $\text{YSi}_2\text{Al}_2\text{O}_x$. This is similar to the composition of the liquid phase reported in the Y_2O_3 - SiO_2 - Al_2O_3 phase diagram [12] and that is present at $\approx 1400^\circ\text{C}$. Although this area of the phase diagram has not been fully evaluated, no crystalline Y-Si-Al-O material has been determined to exist, supporting the idea that this is an amorphous phase. Only traces of Y were detected in the mullite phase.

TEM analysis of sintered specimens confirmed the presence of an amorphous phase along the grain boundaries of as-sintered specimens and crystalline $\text{Y}_2\text{Si}_2\text{O}_7$ at triple points in annealed specimens (Fig. 5). Transformation of the $\text{Y}_2\text{Si}_2\text{O}_7$ from amorphous to crystalline has been shown to significantly increase the strength of Si_3N_4 , although no mechanism for the effect was provided [14]. Crystallizing the $\text{Y}_2\text{Si}_2\text{O}_7$ phase in mullite may produce an increase in strength.

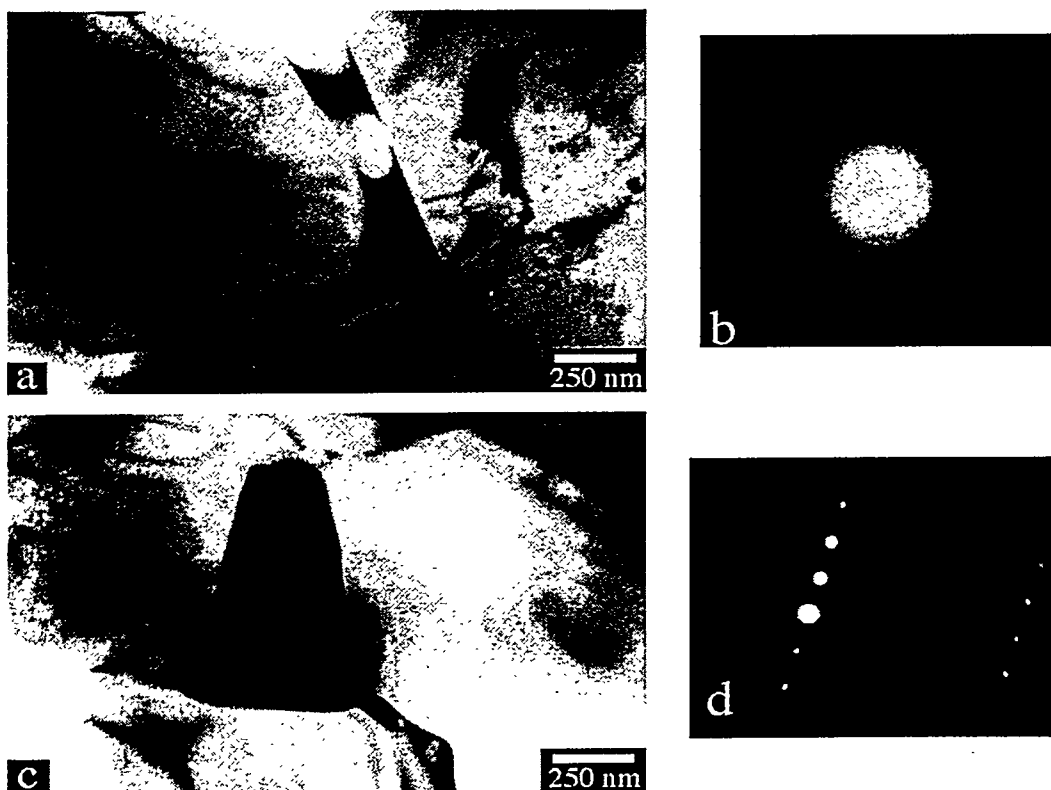


Figure 5. TEM analysis of mullite-5 wt.% Y_2O_3 : (a) as sintered, (b) electron diffraction pattern of amorphous grain-boundary phase, (c) after annealing, and (d) electron diffraction pattern of crystalline $\text{Y}_2\text{Si}_2\text{O}_7$ phase at triple point.

DTA of the mullite-5 wt.% Y_2O_3 showed endothermic reactions at ≈ 1175 , 1375 , and 1425°C . A reaction at 1375°C was reported by Hwang and Fang [10-11] to be a phase transformation of the $\text{Y}_2\text{Si}_2\text{O}_7$, although in pure $\text{Y}_2\text{Si}_2\text{O}_7$ this transformation should occur at 1225°C [18]. The reactions at 1375 and 1425°C are probably the result of formation of an yttrium aluminosilicate liquid phase, as seems to be indicated by the phase diagram [12]. More work is needed to properly characterize this system.

We could not find information on thermal expansion of $\text{Y}_2\text{Si}_2\text{O}_7$. Specimens that were $\approx 73\%$ dense were prepared, and the average value of α was obtained. Specimens were sintered at 1550°C for 3 h; some were then cooled to room temperature, while others were annealed at 1300°C for 24 h or 1175°C for 24 h. XRD identified all specimens as $\gamma\text{-Y}_2\text{Si}_2\text{O}_7$. The average α from 25 to 1200°C was determined to be $4.5 \times 10^{-6} \text{ cm/cm}^\circ\text{C}$. At $\approx 1225^\circ\text{C}$, there was an increase in the slope, which may indicate a phase transformation. This is the temperature at which an $\alpha\text{-}\beta$ phase transformation should occur, although neither phase was indicated by X-ray diffraction as being present. It may be that a metastable γ phase transforms to β at this temperature. More work will be needed to determine the exact reaction. Trusty et al. [17] reported the room-temperature strength of $\text{Y}_2\text{Si}_2\text{O}_7$ to be 219 MPa for a 92% -dense material. The phase of the material was not identified, but based on the theoretical density used, it was probably either β or γ , which have the same theoretical density of 4.03 g/cm^3 . It appears, based on the preliminary data, that $\text{Y}_2\text{Si}_2\text{O}_7$ should be compatible with mullite, each having similar strength and α .

CONCLUSIONS

We conclude from our studies that:

1. Y_2O_3 is effective at reducing the sintering time and temperature needed to achieve highly dense mullite.
2. The addition of 5 wt.% Y_2O_3 to mullite does not significantly affect α .
3. Without doping, under similar processing conditions, mullite will achieve only $\approx 70\%$ of its theoretical density and will have a much lower strength.
4. By proper annealing, the amorphous grain boundary phase can be crystallized.
5. Preliminary analysis of the $\text{Y}_2\text{Si}_2\text{O}_7$ material indicates that in the β and γ forms, $\text{Y}_2\text{Si}_2\text{O}_7$ should be reasonably compatible with mullite.

ACKNOWLEDGMENT

This work was supported by the Defense Advanced Research Projects Agency, through a Department of Energy Interagency Agreement, and Work for Others Contract 82110, under Contract W-31-109-Eng-38.

REFERENCES

¹D. Popovic, G. A. Danko, K. Stuffle, B. H. King, and J. H. Halloran, "Relationship Between Architecture, Flexural Strength, and Work of Fracture fro Fibrous Monolithic Ceramics," pp. 167-174 in Advanced Synthesis of Processing of Composites and Advanced Ceramics (Ceramic Transactions vol. 56), Edited by K. V. Logan, The American Ceramic Society, Westerville, OH (1995).

²D. Kovar, B. H. King, R. W. Trice, and J. W. Halloran, "Fibrous Monolithic Ceramics," Journal of the American Ceramic Society, 80 [10], 2471-87 (1997).

³S. Baskaran, S. D. Nunn, D. Popovic, J. W. Halloran, "Fibrous Monolithic Ceramics: I, Fabrication, Microstructure, and Indentation Behavior," Journal of the American Ceramic Society, 76 [9], 2209-16 (1993).

⁴S. Baskaran and J. W. Halloran, "Fibrous Monolithic Ceramics: II, Flexural Strength and Fracture Behavior of the Silicon Carbide/Graphite System," Journal of the American Ceramic Society, 76 [9], 2217-24 (1993).

⁵G. Hilmas, A. Brady, U. Abdali, G. Zywicki, and J. Halloran, "Fibrous Monoliths: Non-Brittle Fracture from Powder-Processed Ceramics," Materials Science and Engineering A195, 263-268 (1995).

⁶S. Baskaran and J. W. Halloran, "Fibrous Monolithic Ceramics: III, Mechanical Properties and Oxidation Behavior of the Silicon Carbide/Boron Nitride System," Journal of the American Ceramic Society, 77 [5], 1249-55 (1994).

⁷S. H. Hong and G. L. Messing, "Anisotropic Grain Growth in Diphasic-Gel-Derived Titania-Doped Mullite," Journal of the American Ceramic Society, 81 [5] 1269-77 (1998).

⁸T. Mitamura, H. Kobayashi, N. Ishibashi, and T. Akiba, "Effects of Rare Earth Oxide Additions on the Sintering of Mullite," Journal of the Ceramic Society of Japan, International Edition 99, 339-344 (1991).

⁹R. G. Chandran, B. K. Chandrashekhar, C. Ganguly, and K. C. Patil, "Sintering and Microstructural Investigations on Combustion Processed Mullite," Journal of the European Ceramic Society 16, 843-49 (1996).

¹⁰C. Hwang and D. Fang, "Effects of Y_2O_3 Additions on the Sinterability and Microstructure of Mullite (Part I)," Journal of the Ceramic Society of Japan, International Edition 100, 1141-46 (1992).

¹¹D. Fang and C. Hwang, "Effects of Y_2O_3 Additions on the Sinterability and Microstructure of Mullite (Part II)," Journal of the Ceramic Society of Japan, International Edition 101, 322-26 (1993).

¹²U. Kolitsch, H. J. Seifert, T. Ludwig, and F. Aldinger, "Phase Equilibrium and Crystal Chemistry in the Y_2O_3 - Al_2O_3 - SiO_2 System," Journal of Materials Research 14 [2], 447-55 (1999).

¹³R. K. Govila, "Strength Characterization of Yttria-Doped Sintered Silicon Nitride," *Journal of Materials Science* 20, 4345-53 (1985).

¹⁴A. Tsuge, K. Nishida, and M Komatsu, "Effects of Crystallizing the Grain-Boundary Glass Phase on the High-Temperature Strength of Hot-Pressed Si_3N_4 Containing Y_2O_3 ," *Journal of the American Ceramic Society* 58 [7-8], 323-326 (1975).

¹⁵D. R. Clarke and G. Thomas, "Microstructure of Y_2O_3 Fluxed Hot-Pressed Silicon Nitride," *Journal of the American Ceramic Society* 61 [3-4], 114-18 (1978).

¹⁶M. G. M. U. Ismail, Z. Nakai, T. Akiba, and S. Somiya, "Sol-Gel Synthesis and Densification of MgO Doped Mullite Powders," *Ceramic Powder Science III* (Ceramic Transactions Vol. 12), Edited by G. L. Messing, S. Hirano and H. Hausner, The American Ceramic Society, Inc., Westerville, OH (1990).

¹⁷P. A. Trusty, C. B. Ponton, and A. R. Boccaccini, "Fabrication of Woven NicalonTM (NL607) SUC Fibre-Yttrium Disilicate CMCs Using Electrophoretic Deposition," pp 391-398 in *Ceramic Processing Science* (Ceramic Transactions vol. 83), Edited by G. L Messing, F. F. Lange, and S. Hirano, The American Ceramic Society, Westerville, OH (1999).

¹⁸C.H. Drummond III, W. E. Lee, W. A. Sanders, and J. D. Kiser, "Crystallization and Characterization of $\text{Y}_2\text{O}_3\text{-SiO}_2$ Glasses," *Ceramic Engineering and Science Proceedings* 9 [9-10], 1343-54 (1988).